

Search for a Low-Mass Neutral Higgs Boson with Suppressed Couplings to Fermions Using Events with Multiphoton Final States

T. Aaltonen,²¹ S. Amerio^{ll, 39} D. Amidei,³¹ A. Anastassov^{w, 15} A. Annovi,¹⁷ J. Antos,¹² G. Apollinari,¹⁵ J.A. Appel,¹⁵ T. Arisawa,⁵¹ A. Artikov,¹³ J. Asaadi,⁴⁷ W. Ashmanskas,¹⁵ B. Auerbach,² A. Aurisano,⁴⁷ F. Azfar,³⁸ W. Badgett,¹⁵ T. Bae,²⁵ A. Barbaro-Galtieri,²⁶ V.E. Barnes,⁴³ B.A. Barnett,²³ P. Barria^{nn, 41} P. Bartos,¹² M. Bauce^{ll, 39} F. Bedeschi,⁴¹ S. Behari,¹⁵ G. Bellettini^{mm, 41} J. Bellinger,⁵³ D. Benjamin,¹⁴ A. Beretvas,¹⁵ A. Bhatti,⁴⁵ K.R. Bland,⁵ B. Blumenfeld,²³ A. Bocci,¹⁴ A. Bodek,⁴⁴ D. Bortoletto,⁴³ J. Boudreau,⁴² A. Boveia,¹¹ L. Brigliadori^{kk, 6} C. Bromberg,³² E. Brucken,²¹ J. Budagov,¹³ H.S. Budd,⁴⁴ K. Burkett,¹⁵ G. Busetto^{ll, 39} P. Bussey,¹⁹ P. Butti^{mm, 41} A. Buzatu,¹⁹ A. Calamba,¹⁰ S. Camarda,⁴ M. Campanelli,²⁸ F. Canelli^{ee, 11} B. Carls,²² D. Carlsmith,⁵³ R. Carosi,⁴¹ S. Carrillo^{l, 16} B. Casal^{j, 9} M. Casarsa,⁴⁸ A. Castro^{kk, 6} P. Catastini,²⁰ D. Cauz^{sstt, 48} V. Cavaliere,²² A. Cerri^{e, 26} L. Cerrito^{r, 28} Y.C. Chen,¹ M. Chertok,⁷ G. Chiarelli,⁴¹ G. Chlachidze,¹⁵ K. Cho,²⁵ D. Chokheli,¹³ A. Clark,¹⁸ C. Clarke,⁵² M.E. Convery,¹⁵ J. Conway,⁷ M. Corbo^{z, 15} M. Cordelli,¹⁷ C.A. Cox,⁷ D.J. Cox,⁷ M. Cremonesi,⁴¹ D. Cruz,⁴⁷ J. Cuevas^{y, 9} R. Culbertson,¹⁵ N. d'Ascenzo^{v, 15} M. Datta^{hh, 15} P. de Barbaro,⁴⁴ L. Demortier,⁴⁵ M. Deninno,⁶ M. D'Errico^{ll, 39} F. Devoto,²¹ A. Di Canto^{mm, 41} B. Di Ruzza^{p, 15} J.R. Dittmann,⁵ S. Donati^{mm, 41} M. D'Onofrio,²⁷ M. Dorigo^{uu, 48} A. Driutti^{sstt, 48} K. Ebina,⁵¹ R. Edgar,³¹ R. Erbacher,⁷ S. Errede,²² B. Esham,²² S. Farrington,³⁸ J.P. Fernández Ramos,²⁹ R. Field,¹⁶ G. Flanagan^{t, 15} R. Forrest,⁷ M. Franklin,²⁰ J.C. Freeman,¹⁵ H. Frisch,¹¹ Y. Funakoshi,⁵¹ C. Galloni^{mm, 41} A.F. Garfinkel,⁴³ P. Garosi^{nn, 41} H. Gerberich,²² E. Gerchtein,¹⁵ S. Giagu,⁴⁶ V. Giakoumopoulou,³ K. Gibson,⁴² C.M. Ginsburg,¹⁵ N. Giokaris,³ P. Giromini,¹⁷ V. Glagolev,¹³ D. Glenzinski,¹⁵ M. Gold,³⁴ D. Goldin,⁴⁷ A. Golossanov,¹⁵ G. Gomez,⁹ G. Gomez-Ceballos,³⁰ M. Goncharov,³⁰ O. González López,²⁹ I. Gorelov,³⁴ A.T. Goshaw,¹⁴ K. Goulianos,⁴⁵ E. Gramellini,⁶ C. Grosso-Pilcher,¹¹ J. Guimaraes da Costa,²⁰ S.R. Hahn,¹⁵ J.Y. Han,⁴⁴ F. Happacher,¹⁷ K. Hara,⁴⁹ M. Hare,⁵⁰ R.F. Harr,⁵² T. Harrington-Taber^{m, 15} K. Hatakeyama,⁵ C. Hays,³⁸ J. Heinrich,⁴⁰ M. Herndon,⁵³ A. Hocker,¹⁵ Z. Hong,⁴⁷ W. Hopkins^{f, 15} S. Hou,¹ R.E. Hughes,³⁵ U. Husemann,⁵⁴ M. Hussein^{cc, 32} J. Huston,³² G. Introzzi^{ppqq, 41} M. Iori^{rr, 46} A. Ivanov^{o, 7} E. James,¹⁵ D. Jang,¹⁰ B. Jayatilaka,¹⁵ E.J. Jeon,²⁵ S. Jindariani,¹⁵ M. Jones,⁴³ K.K. Joo,²⁵ S.Y. Jun,¹⁰ T.R. Junk,¹⁵ M. Kambeitz,²⁴ T. Kamon,^{25, 47} P.E. Karchin,⁵² A. Kasmai,⁵ Y. Kato^{n, 37} W. Ketchum^{ii, 11} J. Keung,⁴⁰ B. Kilminster^{ee, 15} D.H. Kim,²⁵ H.S. Kim^{bb, 15} J.E. Kim,²⁵ M.J. Kim,¹⁷ S.H. Kim,⁴⁹ S.B. Kim,²⁵ Y.J. Kim,²⁵ Y.K. Kim,¹¹ N. Kimura,⁵¹ M. Kirby,¹⁵ K. Knoepfel,¹⁵ K. Kondo,^{51, *} D.J. Kong,²⁵ J. Konigsberg,¹⁶ A.V. Kotwal,¹⁴ M. Kreps,²⁴ J. Kroll,⁴⁰ M. Kruse,¹⁴ T. Kuhr,²⁴ M. Kurata,⁴⁹ A.T. Laasanen,⁴³ S. Lammel,¹⁵ M. Lancaster,²⁸ K. Lannon^{x, 35} G. Latino^{nn, 41} H.S. Lee,²⁵ J.S. Lee,²⁵ S. Leo,²² S. Leone,⁴¹ J.D. Lewis,¹⁵ A. Limosani^{s, 14} E. Lipeles,⁴⁰ A. Lister^{a, 18} Q. Liu,⁴³ T. Liu,¹⁵ S. Lockwitz,⁵⁴ A. Loginov,⁵⁴ D. Lucchesi^{ll, 39} A. Lucà,¹⁷ J. Lueck,²⁴ P. Lujan,²⁶ P. Lukens,¹⁵ G. Lungu,⁴⁵ J. Lys,²⁶ R. Lysak^{d, 12} R. Madrak,¹⁵ P. Maestro^{nn, 41} S. Malik,⁴⁵ G. Manca^{b, 27} A. Manousakis-Katsikakis,³ L. Marchese^{jj, 6} F. Margaroli,⁴⁶ P. Marino^{oo, 41} K. Matera,²² M.E. Mattson,⁵² A. Mazzacane,¹⁵ P. Mazzanti,⁶ R. McNulty^{i, 27} A. Mehta,²⁷ P. Mehtala,²¹ C. Mesropian,⁴⁵ T. Miao,¹⁵ D. Mietlicki,³¹ A. Mitra,¹ H. Miyake,⁴⁹ S. Moed,¹⁵ N. Moggi,⁶ C.S. Moon^{z, 15} R. Moore^{ffgg, 15} M.J. Morello^{oo, 41} A. Mukherjee,¹⁵ Th. Muller,²⁴ P. Murat,¹⁵ M. Mussini^{kk, 6} J. Nachtman^{m, 15} Y. Nagai,⁴⁹ J. Naganoma,⁵¹ I. Nakano,³⁶ A. Napier,⁵⁰ J. Nett,⁴⁷ T. Nigmanov,⁴² L. Nodulman,² S.Y. Noh,²⁵ O. Normiella,²² L. Oakes,³⁸ S.H. Oh,¹⁴ Y.D. Oh,²⁵ T. Okusawa,³⁷ R. Orava,²¹ L. Ortolan,⁴ C. Pagliarone,⁴⁸ E. Palencia^{e, 9} P. Palmi,³⁴ V. Papadimitriou,¹⁵ W. Parker,⁵³ G. Pauletta^{sstt, 48} M. Paulini,¹⁰ C. Paus,³⁰ T.J. Phillips,¹⁴ G. Piacentino^{g, 15} E. Pianori,⁴⁰ J. Pilot,⁷ K. Pitts,²² C. Plager,⁸ L. Pondrom,⁵³ S. Poprocki^{f, 15} K. Potamianos,²⁶ A. Pranko,²⁶ F. Prokoshin^{aa, 13} F. Ptohos^{g, 17} G. Punzi^{mm, 41} I. Redondo Fernández,²⁹ P. Renton,³⁸ M. Rescigno,⁴⁶ F. Rimondi,^{6, *} L. Ristori,^{41, 15} A. Robson,¹⁹ T. Rodriguez,⁴⁰ S. Rolli^{h, 50} M. Ronzani^{mm, 41} R. Roser,¹⁵ J.L. Rosner,¹¹ F. Ruffini^{nn, 41} A. Ruiz,⁹ J. Russ,¹⁰ V. Rusu,¹⁵ W.K. Sakumoto,⁴⁴ Y. Sakurai,⁵¹ L. Santi^{sstt, 48} K. Sato,⁴⁹ V. Saveliev^{v, 15} A. Savoy-Navarro^{z, 15} P. Schlabach,¹⁵ E.E. Schmidt,¹⁵ T. Schwarz,³¹ L. Scodellaro,⁹ F. Scuri,⁴¹ S. Seidel,³⁴ Y. Seiya,³⁷ A. Semenov,¹³ F. Sforza^{mm, 41} S.Z. Shalhout,⁷ T. Shears,²⁷ P.F. Shepard,⁴² M. Shimojima^{u, 49} M. Shochet,¹¹ I. Shreyber-Tecker,³³ A. Simonenko,¹³ K. Sliwa,⁵⁰ J.R. Smith,⁷ F.D. Snider,¹⁵ H. Song,⁴² V. Sorin,⁴ R. St. Denis,^{19, *} M. Stancari,¹⁵ D. Stentz^{w, 15} J. Strologas,³⁴ Y. Sudo,⁴⁹ A. Sukhanov,¹⁵ I. Suslov,¹³ K. Takemasa,⁴⁹ Y. Takeuchi,⁴⁹ J. Tang,¹¹ M. Tecchio,³¹ P.K. Teng,¹ J. Thom^{f, 15} E. Thomson,⁴⁰ V. Thukral,⁴⁷ D. Toback,⁴⁷ S. Tokar,¹² K. Tollefson,³² T. Tomura,⁴⁹ D. Tonelli^{e, 15} S. Torre,¹⁷ D. Torretta,¹⁵ P. Totaro,³⁹ M. Trovato^{oo, 41} F. Ukegawa,⁴⁹ S. Uozumi,²⁵ F. Vázquez^{l, 16} G. Velev,¹⁵

C. Vellidis,¹⁵ C. Vernieri^{oo},⁴¹ M. Vidal,⁴³ R. Vilar,⁹ J. Vizán^{dd},⁹ M. Vogel,³⁴ G. Volpi,¹⁷ P. Wagner,⁴⁰ R. Wallny^j,¹⁵ S.M. Wang,¹ D. Waters,²⁸ W.C. Wester III,¹⁵ D. Whiteson^c,⁴⁰ A.B. Wicklund,² S. Wilbur,⁷ H.H. Williams,⁴⁰ J.S. Wilson,³¹ P. Wilson,¹⁵ B.L. Winer,³⁵ P. Wittich^f,¹⁵ S. Wolbers,¹⁵ H. Wolfe,³⁵ T. Wright,³¹ X. Wu,¹⁸ Z. Wu,⁵ K. Yamamoto,³⁷ D. Yamato,³⁷ T. Yang,¹⁵ U.K. Yang,²⁵ Y.C. Yang,²⁵ W.-M. Yao,²⁶ G.P. Yeh,¹⁵ K. Yi^m,¹⁵ J. Yoh,¹⁵ K. Yorita,⁵¹ T. Yoshida^k,³⁷ G.B. Yu,¹⁴ I. Yu,²⁵ A.M. Zanetti,⁴⁸ Y. Zeng,¹⁴ C. Zhou,¹⁴ and S. Zucchelli^{kk6}

(CDF Collaboration)[†]

¹*Institute of Physics, Academia Sinica, Taipei, Taiwan 11529, Republic of China*

²*Argonne National Laboratory, Argonne, Illinois 60439, USA*

³*University of Athens, 157 71 Athens, Greece*

⁴*Institut de Física d'Altes Energies, ICREA, Universitat Autònoma de Barcelona, E-08193, Bellaterra (Barcelona), Spain*

⁵*Baylor University, Waco, Texas 76798, USA*

⁶*Istituto Nazionale di Fisica Nucleare Bologna, ^{kk}University of Bologna, I-40127 Bologna, Italy*

⁷*University of California, Davis, Davis, California 95616, USA*

⁸*University of California, Los Angeles, Los Angeles, California 90024, USA*

⁹*Instituto de Física de Cantabria, CSIC-University of Cantabria, 39005 Santander, Spain*

¹⁰*Carnegie Mellon University, Pittsburgh, Pennsylvania 15213, USA*

¹¹*Enrico Fermi Institute, University of Chicago, Chicago, Illinois 60637, USA*

¹²*Comenius University, 842 48 Bratislava, Slovakia; Institute of Experimental Physics, 040 01 Kosice, Slovakia*

¹³*Joint Institute for Nuclear Research, RU-141980 Dubna, Russia*

¹⁴*Duke University, Durham, North Carolina 27708, USA*

¹⁵*Fermi National Accelerator Laboratory, Batavia, Illinois 60510, USA*

¹⁶*University of Florida, Gainesville, Florida 32611, USA*

¹⁷*Laboratori Nazionali di Frascati, Istituto Nazionale di Fisica Nucleare, I-00044 Frascati, Italy*

¹⁸*University of Geneva, CH-1211 Geneva 4, Switzerland*

¹⁹*Glasgow University, Glasgow G12 8QQ, United Kingdom*

²⁰*Harvard University, Cambridge, Massachusetts 02138, USA*

²¹*Division of High Energy Physics, Department of Physics, University of Helsinki,*

FIN-00014, Helsinki, Finland; Helsinki Institute of Physics, FIN-00014, Helsinki, Finland

²²*University of Illinois, Urbana, Illinois 61801, USA*

²³*The Johns Hopkins University, Baltimore, Maryland 21218, USA*

²⁴*Institut für Experimentelle Kernphysik, Karlsruhe Institute of Technology, D-76131 Karlsruhe, Germany*

²⁵*Center for High Energy Physics: Kyungpook National University,*

Daegu 702-701, Korea; Seoul National University, Seoul 151-742,

Korea; Sungkyunkwan University, Suwon 440-746,

Korea; Korea Institute of Science and Technology Information,

Daejeon 305-806, Korea; Chonnam National University,

Gwangju 500-757, Korea; Chonbuk National University, Jeonju 561-756,

Korea; Ewha Womans University, Seoul, 120-750, Korea

²⁶*Ernest Orlando Lawrence Berkeley National Laboratory, Berkeley, California 94720, USA*

²⁷*University of Liverpool, Liverpool L69 7ZE, United Kingdom*

²⁸*University College London, London WC1E 6BT, United Kingdom*

²⁹*Centro de Investigaciones Energeticas Medioambientales y Tecnológicas, E-28040 Madrid, Spain*

³⁰*Massachusetts Institute of Technology, Cambridge, Massachusetts 02139, USA*

³¹*University of Michigan, Ann Arbor, Michigan 48109, USA*

³²*Michigan State University, East Lansing, Michigan 48824, USA*

³³*Institution for Theoretical and Experimental Physics, ITEP, Moscow 117259, Russia*

³⁴*University of New Mexico, Albuquerque, New Mexico 87131, USA*

³⁵*The Ohio State University, Columbus, Ohio 43210, USA*

³⁶*Okayama University, Okayama 700-8530, Japan*

³⁷*Osaka City University, Osaka 558-8585, Japan*

³⁸*University of Oxford, Oxford OX1 3RH, United Kingdom*

³⁹*Istituto Nazionale di Fisica Nucleare, Sezione di Padova, ^{ll}University of Padova, I-35131 Padova, Italy*

⁴⁰*University of Pennsylvania, Philadelphia, Pennsylvania 19104, USA*

⁴¹*Istituto Nazionale di Fisica Nucleare Pisa, ^{mm}University of Pisa,*

ⁿⁿUniversity of Siena, ^{oo}Scuola Normale Superiore,

I-56127 Pisa, Italy, ^{pp}INFN Pavia, I-27100 Pavia,

Italy, ^{qq}University of Pavia, I-27100 Pavia, Italy

⁴²*University of Pittsburgh, Pittsburgh, Pennsylvania 15260, USA*

⁴³*Purdue University, West Lafayette, Indiana 47907, USA*

⁴⁴*University of Rochester, Rochester, New York 14627, USA*

⁴⁵*The Rockefeller University, New York, New York 10065, USA*

⁴⁶*Istituto Nazionale di Fisica Nucleare, Sezione di Roma 1,*

^{rr}Sapienza Università di Roma, I-00185 Roma, Italy

⁴⁷*Mitchell Institute for Fundamental Physics and Astronomy,*

Texas A&M University, College Station, Texas 77843, USA

⁴⁸*Istituto Nazionale di Fisica Nucleare Trieste, ^{ss}Gruppo Collegato di Udine,*

^{tt}University of Udine, I-33100 Udine, Italy, ^{uu}University of Trieste, I-34127 Trieste, Italy

⁴⁹*University of Tsukuba, Tsukuba, Ibaraki 305, Japan*

⁵⁰*Tufts University, Medford, Massachusetts 02155, USA*

⁵¹*Waseda University, Tokyo 169, Japan*

⁵²*Wayne State University, Detroit, Michigan 48201, USA*

⁵³*University of Wisconsin-Madison, Madison, Wisconsin 53706, USA*

⁵⁴*Yale University, New Haven, Connecticut 06520, USA*

(Dated: June 2, 2016)

A search for a Higgs boson with suppressed couplings to fermions, h_f , assumed to be the neutral, lower-mass partner of the Higgs boson discovered at the Large Hadron Collider, is reported. Such a Higgs boson could exist in extensions of the standard model with two Higgs doublets, and could be produced via $p\bar{p} \rightarrow H^\pm h_f \rightarrow W^* h_f h_f \rightarrow 4\gamma + X$, where H^\pm is a charged Higgs boson. This analysis uses all events with at least three photons in the final state from proton-antiproton collisions at a center-of-mass energy of 1.96 TeV collected by the Collider Detector at Fermilab, corresponding to an integrated luminosity of 9.2 fb^{-1} . No evidence of a signal is observed in the data. Values of Higgs-boson masses between 10 and 100 GeV/c^2 are excluded at 95% Bayesian credibility.

PACS numbers: 12.60.Fr, 13.85.Rm, 14.80.Ec, 14.80.Fd

In the standard model (SM) of particle physics, the masses of elementary particles are generated by the spontaneous breaking of the electroweak gauge symmetry [1], which predicts the existence of the Higgs boson. In 2012, the ATLAS and CMS experiments at CERN's Large Hadron Collider (LHC) discovered a scalar boson with mass of approximately $125 \text{ GeV}/c^2$ and properties consistent with those expected for the SM Higgs boson [2, 3]. Some evidence for such a boson had also been presented by the Tevatron experiments [4]. The detailed phenomenology of the Higgs boson is, however, yet to be investigated. The possibility that the recently observed Higgs boson is part of an extended Higgs sector is attractive because it would address some relevant open questions about the SM such as the generation of matter-antimatter asymmetry in the Universe [5] and it is not ruled out experimentally.

A minimal extension, the “two-Higgs-doublet model” (2HDM) [6], assumes two doublets of Higgs fields. The resulting particle spectrum for the CP -conserving case consists of three electrically neutral Higgs bosons, h^0 , H^0 and A^0 , and two charged Higgs-bosons, H^+ , H^- , where h^0 is less massive than H^0 . The acronym CP represents the combined operations of charge-conjugation and parity transformation. An important parameter for predictions from the model is the ratio $\tan\beta$ of the two vacuum-expectation values for the neutral components of the two Higgs doublets. Assuming that the boson discovered recently at the LHC is the h^0 , searches for additional, more-massive neutral Higgs bosons were performed [7, 8], yielding exclusion limits on production cross sections.

In this Letter, we consider an alternative case in which the newly-discovered boson corresponds to the high-mass H^0 and the lower-mass h^0 is yet to be observed. This scenario is poorly constrained experimentally if $\tan\beta$ is large and h^0 has suppressed couplings to fermions at leading order. The h^0 is referred to as the fermiophobic Higgs boson (h_f). Searches performed at various experiments [9–11] have set lower bounds of its mass, m_{h_f} , at 100–150 GeV/c^2 . These mass limits, however, were obtained assuming simplified models in which the couplings between the h_f and electroweak-gauge bosons are of the same strength as those in the SM, which is not necessarily true in the 2HDM, as they may be strongly suppressed when $\tan\beta$ is large [12], by a factor of approximately 10^{-2} when $\tan\beta = 10$, for example. A low-mass h_f ($m_{h_f} \lesssim 100 \text{ GeV}/c^2$), therefore, could have eluded the previous searches if $\tan\beta$ is large. To fill this gap in exploring the Higgs sector, we focus on the process $q\bar{q}' \rightarrow W^* \rightarrow h_f H^\pm$, followed by the decay $H^\pm \rightarrow h_f W^*$, where q and \bar{q}' are quarks and antiquarks in the colliding protons and antiprotons taking part in the hard interaction, and W^* represents a virtual W boson. This process, involving H^\pm , has enhanced production rates for large $\tan\beta$ [13]. By assuming no couplings to fermions, the branching fraction (\mathcal{B}) of h_f decays to two photons, $h_f \rightarrow \gamma\gamma$, is near 100% for $m_{h_f} \lesssim 95 \text{ GeV}/c^2$ [13, 14]. The production of two h_f particles could result in a distinctive multiphoton topology with small background rates. The couplings of the H^0 to SM particles in this scenario are similar to those of the SM Higgs boson [13] and we perform the analysis assuming that its mass, m_{H^0} ,

is $125 \text{ GeV}/c^2$. The decay of $H^0 \rightarrow h_f h_f$, when it is kinematically allowed and when the coupling is sizable, can also lead to multiphoton final states. We conservatively neglect this contribution to the expected signal. We also assume the A^0 mass, m_{A^0} , to be $350 \text{ GeV}/c^2$, large enough so as not to contribute to H^\pm decays – the specific choice of m_{A^0} has little effect on the final result, and we take $\tan\beta = 10$. The expected production cross section multiplied by the appropriate branching fractions ranges approximately from 100 pb to 10 fb for the explored m_{h_f} and the H^\pm mass (m_{H^\pm}) values, from 10 to 105 GeV/c^2 and from 30 to 300 GeV/c^2 , respectively.

This analysis is based on the entire data set of proton-antiproton collisions at a center-of-mass energy of 1.96 TeV collected with the Collider Detector at Fermilab (CDF II) between February 2002 and September 2011, corresponding to an integrated luminosity of 9.2 fb^{-1} . We select events with multiple photon candidates by applying criteria optimized for achieving the best sensitivity. We compare the observed event yields with background expectations, which are evaluated using a combination of Monte Carlo (MC) simulation and experimental data. A challenge is to estimate the contribution from background events containing clusters of particles (jets) misidentified as photons.

CDF II is a general-purpose detector consisting of tracking devices in a 1.4 T axial magnetic field, surrounded by calorimeters with a projective-tower geometry, and muon detectors surrounding the calorimeters. Gas proportional wire chambers with cathode strips (shower-maximum strip detectors) are located at a depth approximately corresponding to the maximum development of typical electromagnetic (EM) showers to measure precisely their centroid position and shape in the plane transverse to the shower development. Detailed descriptions of the CDF II detector are in Ref. [15].

The initial data sample is obtained using a real-time event-selection system (trigger) that requires either two EM-energy clusters in the calorimeter, each with $E_T \equiv E \sin\theta > 12 \text{ GeV}$, or three clusters, each with $E_T > 10 \text{ GeV}$, where E is the cluster energy measured with the calorimeter, θ is the polar angle, and E_T is the transverse energy [16]. In the analysis, we select events with at least three EM-energy clusters with $E_T > 15 \text{ GeV}$. They must be located in the central detector (pseudorapidity magnitude $|\eta| < 1.1$) [16], where reliable tracking of charged particles is available [17]. The photons are also required to be isolated: additional calorimeter E_T in a cone of angular radius $R = \sqrt{(\Delta\eta)^2 + (\Delta\phi)^2} = 0.4$ [16] around the photon candidate must be less than 2 GeV, and the scalar sum of transverse momenta of charged particles in the same cone must be less than 2 GeV/c . We then apply photon-identification criteria based on the EM-shower profile, which must be consistent with the ex-

pectation for an isolated photon [18]. For photons with $E_T > 15 \text{ GeV}$ in a fiducial region of the central detector, the probability to pass all selections is 80–90%.

We estimate the reconstruction efficiency for signal events as a function of m_{h_f} and m_{H^\pm} using PYTHIA (version 6.4) MC simulation [19]. The generated events are passed through the full detector simulation based on GEANT [20]. The simulation of the EM response of the detector is calibrated by matching the observed energies in samples of $Z \rightarrow e^+e^-$ events in the data and the MC simulation [18]. The fractions of generated signal events to pass all event selections are in the range 1–10% depending on m_{h_f} and m_{H^\pm} .

Direct triphoton production is a major source of background events. We predict the kinematic distributions from simulated data generated with MADGRAPH (version 5) interfaced with MADEVENT [21] and combined with parton showering from PYTHIA. MADGRAPH provides direct triphoton production with up to two additional jets. The renormalization and factorization scales are set to the sum of the squares of the photons' transverse momenta. The generated events are passed through the full detector simulation and we apply the same photon selection as that used for data.

Another source of background is the production of events with jets misidentified as photons. This background includes photons produced in the fragmentation process of quarks or gluons to hadrons. For estimating this contribution, we introduce a loose photon selection which simply collects EM-energy clusters without any associated tracks. In a sample of three-photon candidates selected with the loose selection, there are eight possible combinations of E_T -ordered photons and EM-like jets, $\gamma\gamma\gamma, \gamma\gamma j, \dots$, where j represents an EM-like jet. The numbers of these events are unknown and we express them by a vector \mathbf{n}^* of event counts ($n_{\gamma\gamma\gamma}^*, n_{\gamma\gamma j}^*, \dots$). By applying the full set of criteria for the photon selection, we categorize the events in eight classes depending on whether each of the photon candidates in a given event passes (p) or fails (f) the full photon selection (n_{ppp}, n_{ppf}, \dots), denoted by \mathbf{n} . The components of \mathbf{n}^* are obtained by solving eight linear equations $\mathbf{n} = \mathbf{E}\mathbf{n}^*$, where \mathbf{E} is an 8×8 matrix, the elements of which are calculated from the probability for a genuine photon or jet that meets the loose selection to also meet the full photon selection. Once \mathbf{n}^* is obtained by inverting the matrix \mathbf{E} , we estimate the misidentified-jet contribution to n_{ppp} using \mathbf{E} and the calculated elements of \mathbf{n}^* except $n_{\gamma\gamma\gamma}^*$. Statistical uncertainties are propagated to \mathbf{n}^* . The photon efficiencies are measured with the PYTHIA MC and detector simulation, with a final calibration derived by comparing unbiased electrons in $Z \rightarrow e^+e^-$ events in the data and the MC simulation. We estimate the probability for misidentifying jets as photons as a function of E_T

using isolated jets in data samples collected with inclusive jet triggers. We correct for contributions of genuine photons to the set of objects passing the photon selection in the jet samples based on the differences in the expected distributions of isolation and shower shape variables [18]. Genuine photons tend to be isolated and to have good χ^2 values for the comparison of the observed and expected shower shapes, while misidentified jets show broad distributions in both quantities. These differences enable us to extrapolate the amount of misidentified jets from regions of larger isolation and χ^2 values to the region selected by the photon identification. The fraction of misidentified jets is then estimated to be approximately 30% using the calorimetry-based isolation. The misidentification probability varies from a few percent to 25% depending on the E_T .

A third source of background events arises from electroweak processes containing $Z(\rightarrow ee)\gamma$, $W(\rightarrow e\nu)\gamma$, $Z(\rightarrow \tau\tau)\gamma$, or $W(\rightarrow \tau\nu)\gamma$ decays with additional misidentified jets or other photon-like particles that result in the $\gamma\gamma\gamma$ signature. We predict these backgrounds using PYTHIA MC and detector simulation, after normalizing the cross sections to observed W and Z yields in the data.

The total expected number of background events at this stage is 10.3 ± 0.2 , where the uncertainty is statistical. We observe 10 events in the data, which is consistent with the background expectation. None of the observed events contains four or more photons.

In order to further improve the search sensitivity, we apply an additional criterion on the summed E_T of the two highest- E_T photons, $E_T^{\gamma_1} + E_T^{\gamma_2}$. To quantify the search sensitivity, we calculate Bayesian [22] expected limits on the product of the cross section and the branching fraction

$$\sigma(p\bar{p} \rightarrow h_f H^\pm) \times \mathcal{B}(H^\pm \rightarrow h_f W^*) \times [\mathcal{B}(h_f \rightarrow \gamma\gamma)]^2,$$

with respect to theoretical predictions by integrating posterior probability density functions based on predicted number of background events. We assume a uniform prior probability density for the signal rate. The theoretical cross sections at leading order are computed using PYTHIA with an enhancement factor of 1.4 to approximate higher-order contributions. This factor is taken to be the ratio of the W boson production cross section measured by CDF [17] to the corresponding prediction by PYTHIA. This is similar to a calculation of the ratio of the next-to-leading-order prediction to the leading-order prediction of 1.3 ± 0.3 for Higgs boson pair production in Drell-Yan-like processes at the LHC [23], and we note that the central values, which are expected to be similar, are within the theoretical uncertainty on the Higgs boson pair production prediction, which is much larger than the experimental uncertainty on the W boson en-

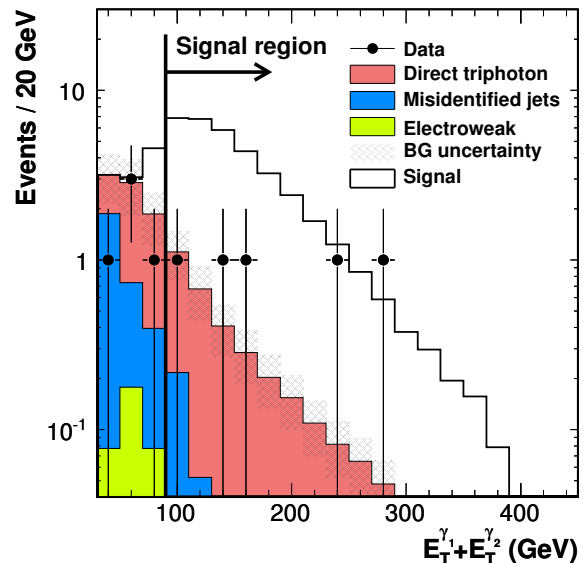


FIG. 1. Distribution of $E_T^{\gamma_1} + E_T^{\gamma_2}$ in events containing three or more photons for data, SM background prediction, and hypothetical signal for a signal point having $m_{h_f} = 75$ GeV/ c^2 and $m_{H^\pm} = 120$ GeV/ c^2 .

hancement factor. Because the h_f signal production process under study begins with W boson production, we use the measured W boson production enhancement factor, but we use the uncertainty on the theoretical prediction, ± 0.3 , as an estimate of the uncertainty in extrapolating the enhancement factor from one process to the other. The branching fractions are calculated with the 2HDMC program (version 1.6.5) [24]. The expected limit is the median in a large set of simulated experiments based on the Poisson fluctuation of the background events. We choose $E_T^{\gamma_1} + E_T^{\gamma_2} > 90$ GeV as the final requirement because it provides the best expected limit. Figure 1 shows the predicted and observed distributions of $E_T^{\gamma_1} + E_T^{\gamma_2}$ and includes the requirement defining the signal region. We compare the background distribution and the expected signal distribution for a signal point having $m_{h_f} = 75$ GeV/ c^2 and $m_{H^\pm} = 120$ GeV/ c^2 .

The main systematic uncertainty on the signal efficiency comes from that on the estimation of the identification efficiency for three photons, which is 8% of the total efficiency based on studies comparing $Z \rightarrow e^+e^-$ in data and simulation [18] by assuming full correlation among three photons. Other sources of systematic uncertainties include those on the parton momentum distributions in the colliding hadrons, the initial- and final-state radiation of a gluon, and the renormalization scale, which are each found to contribute less than 3% of the

TABLE I. Expected number of background events compared to the observed number of events after the final event selection. The first contribution to the uncertainty is statistical and the second is systematic.

	Events in signal region ($E_T^{\gamma 1} + E_T^{\gamma 2} > 90$ GeV)			
Direct triphoton	2.60	\pm	0.04	\pm 0.93
Misidentified jets	0.32	\pm	0.07	\pm 0.17
Electroweak	0.04	\pm	0.01	\pm 0.03
Total	2.96	\pm	0.08	\pm 0.94
Data	5			

total efficiency [18].

We compare the MADGRAPH cross section with MCFM [25] calculations that take into account different higher-order contributions and take the resulting difference of 0.83 events as a systematic uncertainty on the yield of direct triphoton events. The systematic uncertainty from the renormalization scale, that from the initial- and final-state radiation, and that from the luminosity measurement [26] range from 0.16 to 0.21 events. We estimate the total systematic uncertainty on the expected yield of events with misidentified jets to be 0.17 events, which includes the contribution from the measurement of the misidentified-jet probability and that from the possible difference of the probabilities between jets originating from quarks and gluons. The dominant uncertainty on the electroweak contribution originates from the limited size of the simulated event samples used to estimate the small probability to find an extra photon-like particle in the $W(\rightarrow e\nu)\gamma$ events.

Table I shows the expected number of background events and the number of events found in data after the final selection. We find 5 candidate events in data, which is consistent with the expected number of background events.

We check the background predictions using background-rich control samples. In events containing one lower-quality photon candidate that passes the loose selection but fails the full selection, the predicted and observed numbers of events are 372 ± 68 and 370, respectively. In events with $E_T^{\gamma 1} + E_T^{\gamma 2} < 90$ GeV, 6.6 ± 1.7 events are predicted and 5 events observed. The observed agreement supports the reliability of the background estimation.

We perform a Bayesian limit calculation restricted to events observed in the signal region, $E_T^{\gamma 1} + E_T^{\gamma 2} > 90$ GeV, as a function of m_{h_f} , ranging from 10 to 105 GeV/ c^2 , and m_{H^\pm} , ranging from 30 to 300 GeV/ c^2 . We include systematic uncertainties due to the signal ef-

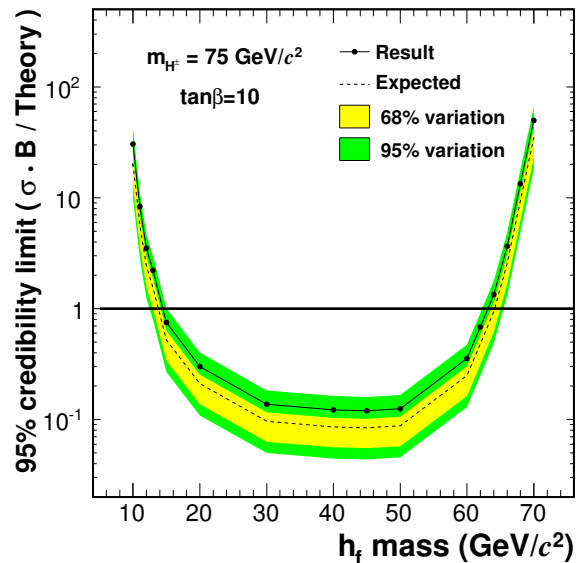


FIG. 2. Upper limit at 95% credibility on the cross-section ratio with respect to theory predictions, calculated for the final selection, including the $E_T^{\gamma 1} + E_T^{\gamma 2} > 90$ GeV requirement. The solid line is the obtained limit, the dashed line is the expected limit, and the shaded regions cover the 68% and 95% of possible variations of expected limit values based on the Poisson statistics of the expected number of background events.

iciency, the predicted number of background events, and the luminosity, as well as the theoretical uncertainty of 20% on the cross section of Higgs boson production [23]. Figure 2 shows the expected and the observed cross section limits at 95% credibility for a particular choice of m_{h_f} and m_{H^\pm} , with possible variations of the expected limits obtained by assuming 68% or 95% of Poisson fluctuations of the number of background events. From Fig. 2, the m_{h_f} region between 14 and 62 GeV/ c^2 is excluded for $m_{H^\pm} = 75$ GeV/ c^2 . Connecting the boundary regions of the excluded m_{h_f} region for various values of m_{H^\pm} in the m_{h_f} vs. m_{H^\pm} plane, we form contours of the excluded mass regions and present them in Fig. 3. The region of parameters given by m_{h_f} between 10 and 100 GeV/ c^2 and m_{H^\pm} between 30 and 170 GeV/ c^2 is excluded. The result does not change significantly if we repeat the analysis by assuming $\tan \beta = 30$, while the excluded region shrinks by approximately 20 GeV/ c^2 for both of m_{h_f} and m_{H^\pm} for $\tan \beta = 3$.

In conclusion, we report on a search for the fermiophobic Higgs boson in the two-Higgs-doublet model using events with at least three photons in the final state, resulting from the hypothetical process $p\bar{p} \rightarrow h_f H^\pm$ followed by $H^\pm \rightarrow h_f W^*$ and $h_f \rightarrow \gamma\gamma$. The observed number of

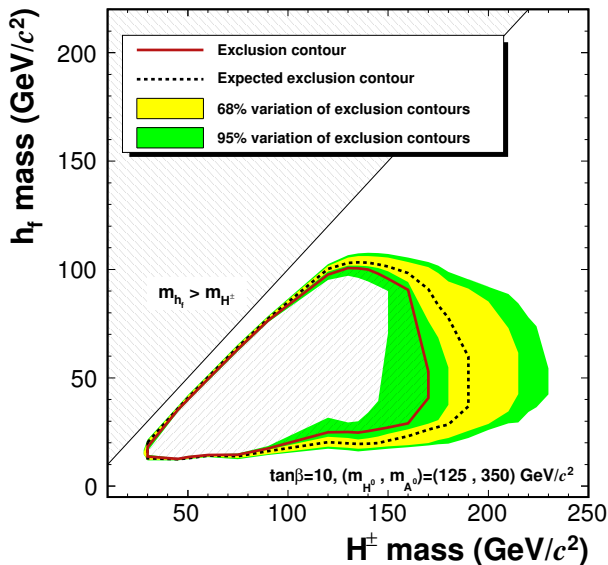


FIG. 3. Excluded mass region at a 95% credibility, calculated for the final selection. The solid curve is the contour enclosing the exclusion region, the dashed line encloses the median expected exclusion region, and the shaded regions cover the 68% and 95% of possible variations of expected contours based on the Poisson statistics of the expected number of background events.

signal candidate events in data is consistent with the expected number of background events. We calculate the upper limit on the product of the cross section and the branching fraction at 95% Bayesian credibility for m_{h_f} values ranging from 10 to 105 GeV/c^2 and for m_{H^\pm} values ranging from 30 to 300 GeV/c^2 , and then translate these limits into an excluded region in the m_{h_f} vs. m_{H^\pm} plane, shown in Fig. 3. The region of parameters given by m_{h_f} between 10 and 100 GeV/c^2 and m_{H^\pm} between 30 and 170 GeV/c^2 is excluded for $\tan\beta = 10$. This is the first search for a fermiophobic neutral Higgs boson with mass smaller than the boson discovered at the LHC in the two-Higgs-doublet model.

We thank the Fermilab staff and the technical staffs of the participating institutions for their vital contributions. This work was supported by the U.S. Department of Energy and National Science Foundation; the Italian Istituto Nazionale di Fisica Nucleare; the Ministry of Education, Culture, Sports, Science and Technology of Japan; the Natural Sciences and Engineering Research Council of Canada; the National Science Council of the Republic of China; the Swiss National Science Foundation; the A.P. Sloan Foundation; the Bundesministerium für Bildung und Forschung, Germany; the Korean World Class University Program, the National Research Foun-

dation of Korea; the Science and Technology Facilities Council and the Royal Society, United Kingdom; the Russian Foundation for Basic Research; the Ministerio de Ciencia e Innovación, and Programa Consolider-Ingenio 2010, Spain; the Slovak R&D Agency; the Academy of Finland; the Australian Research Council (ARC); and the EU community Marie Curie Fellowship Contract No. 302103.

* Deceased

† With visitors from ^aUniversity of British Columbia, Vancouver, BC V6T 1Z1, Canada, ^bIstituto Nazionale di Fisica Nucleare, Sezione di Cagliari, 09042 Monserrato (Cagliari), Italy, ^cUniversity of California Irvine, Irvine, CA 92697, USA, ^dInstitute of Physics, Academy of Sciences of the Czech Republic, 182 21, Czech Republic, ^eCERN, CH-1211 Geneva, Switzerland, ^fCornell University, Ithaca, NY 14853, USA, ^gUniversity of Cyprus, Nicosia CY-1678, Cyprus, ^hOffice of Science, U.S. Department of Energy, Washington, DC 20585, USA, ⁱUniversity College Dublin, Dublin 4, Ireland, ^jETH, 8092 Zürich, Switzerland, ^kUniversity of Fukui, Fukui City, Fukui Prefecture, Japan 910-0017, ^lUniversidad Iberoamericana, Lomas de Santa Fe, México, C.P. 01219, Distrito Federal, ^mUniversity of Iowa, Iowa City, IA 52242, USA, ⁿKinki University, Higashi-Osaka City, Japan 577-8502, ^oKansas State University, Manhattan, KS 66506, USA, ^pBrookhaven National Laboratory, Upton, NY 11973, USA, ^qIstituto Nazionale di Fisica Nucleare, Sezione di Lecce, Via Arnesano, I-73100 Lecce, Italy, ^rQueen Mary, University of London, London, E1 4NS, United Kingdom, ^sUniversity of Melbourne, Victoria 3010, Australia, ^tMuons, Inc., Batavia, IL 60510, USA, ^uNagasaki Institute of Applied Science, Nagasaki 851-0193, Japan, ^vNational Research Nuclear University, Moscow 115409, Russia, ^wNorthwestern University, Evanston, IL 60208, USA, ^xUniversity of Notre Dame, Notre Dame, IN 46556, USA, ^yUniversidad de Oviedo, E-33007 Oviedo, Spain, ^zCNRS-IN2P3, Paris, F-75205 France, ^{aa}Universidad Tecnica Federico Santa Maria, 110v Valparaiso, Chile, ^{bb}Sejong University, Seoul 143-747, Korea, ^{cc}The University of Jordan, Amman 11942, Jordan, ^{dd}Université catholique de Louvain, 1348 Louvain-La-Neuve, Belgium, ^{ee}University of Zürich, 8006 Zürich, Switzerland, ^{ff}Massachusetts General Hospital, Boston, MA 02114 USA, ^{gg}Harvard Medical School, Boston, MA 02114 USA, ^{hh}Hampton University, Hampton, VA 23668, USA, ⁱⁱLos Alamos National Laboratory, Los Alamos, NM 87544, USA, ^{jj}Università degli Studi di Napoli Federico I, I-80138 Napoli, Italy

[1] P. W. Higgs, Phys. Rev. Lett. **13**, 508 (1964).

[2] G. Aad *et al.* (ATLAS Collaboration), Phys. Lett. B **716**, 1 (2012); S. Chatrchyan *et al.* (CMS Collaboration), *ibid.* **716**, 30 (2012); S. Chatrchyan *et al.* (CMS Collaboration), Phys. Rev. Lett. **110**, 081803 (2013); **110**, 189901(E) (2013); G. Aad *et al.* (ATLAS Collaboration), Phys. Lett. B **726**, 120 (2013).

[3] S. Chatrchyan *et al.* (CMS Collaboration), Nature Phys.

- 10**, 557 (2014); G. Aad *et al.* (ATLAS Collaboration), *J. High Energy Phys.* **04** (2015) 117.
- [4] T. Aaltonen *et al.* (CDF and D0 Collaborations), *Phys. Rev. Lett.* **109**, 071804 (2012); T. Aaltonen *et al.* (CDF and D0 Collaborations), *Phys. Rev. D* **88**, 052014 (2013);
- [5] G. C. Branco, P. M. Ferreira, L. Lavoura, M. N. Rebelo, Marc Sher, and João P. Silva, *Phys. Rept.* **516**, 1 (2012), and references therein.
- [6] H. E. Haber, G. L. Kane, and T. Sterling, *Nucl. Phys.* **B161**, 493 (1979).
- [7] T. Aaltonen *et al.* (CDF Collaboration), *Phys. Rev. Lett.* **110**, 121801 (2013).
- [8] V. Khachatryan *et al.* (CMS Collaboration), *Phys. Rev. D* **90**, 112013 (2014).
- [9] V. Lemaitre, in *Proceedings of the 20th Lake Louise Winter Institute, Lake Louise, Alberta, Canada, 2005*, edited by A. Astbury, B. Campbell, F. Khanna, R. Moore, and M. Vincter (World Scientific, Hackensack, 2006), p 199.
- [10] V.M. Abazov *et al.* (D0 Collaboration), *Phys. Rev. Lett.* **107**, 151801 (2011); T. Aaltonen *et al.* (CDF Collaboration), *Phys. Rev. Lett.* **108**, 011801 (2012).
- [11] G. Aad *et al.* (ATLAS Collaboration), *Eur. Phys. J. C* **72**, 2157 (2012); S. Chatrchyan *et al.* (CMS Collaboration), *Phys. Lett. B* **725**, 36 (2013).
- [12] J. F. Gunion, H. E. Haber, G. Kane, and S. Dawson, *The Higgs Hunter's Guide* (Perseus Books, Massachusetts, 1990).
- [13] A. G. Akeroyd, *Nucl. Phys.* **B544**, 557 (1999); A. G. Akeroyd and M. A. Díaz, *Phys. Rev. D* **67**, 095007 (2003); A. G. Akeroyd, A. Alves, M. A. Díaz, and O. Éboli, *Eur. Phys. J. C* **48**, 145 (2006).
- [14] L. Brucher and R. Santos, *Eur. Phys. J. C* **12**, 87 (2000).
- [15] D. Acosta *et al.* (CDF Collaboration), *Phys. Rev. D* **71**, 032001 (2005), and references therein.
- [16] CDF uses a cylindrical coordinate system with $+z$ in the proton beam direction, θ and ϕ are the polar and azimuthal angles, respectively, and η is the pseudorapidity defined by $\eta \equiv -\ln \tan(\theta/2)$.
- [17] A. Abulencia *et al.* (CDF Collaboration), *J. Phys. G* **34**, 2457 (2007).
- [18] T. Aaltonen *et al.* (CDF Collaboration), *Phys. Rev. Lett.* **103**, 061803 (2009), and references therein; T. Aaltonen *et al.* (CDF Collaboration), *Phys. Rev. D* **80**, 111106 (2009), and references therein.
- [19] T. Sjöstrand, P. Edén, C. Friberg, L. Lönnblad, G. Miu, S. Mrenna, and E. Norrbin, *Comput. Phys. Commun.* **135**, 238 (2001).
- [20] R. Brun, F. Carminati, and S. Giani, Technical Report No. CERN-W5013, 1994.
- [21] J. Alwall, R. Frederix, S. Frixione, V. Hirschi, F. Maltoni, O. Mattelaer, H.-S. Shao, T. Stelzer, P. Torrielli, and M. Zaro, *J. High Energy Phys.* **07** (2014) 079.
- [22] K. A. Olive *et al.* (Particle Data Group), *Chin. Phys. C* **38**, 090001 (2014), T. Aaltonen *et al.* (CDF Collaboration), *Phys. Rev. D* **88**, 052013 (2013).
- [23] S. Dawson, E. Eichten, and C. Quigg, *Phys. Rev. D* **31**, 1581 (1985); S. Dawson, S. Dittmaier, and M. Spira, *Phys. Rev. D* **58**, 115012 (1998).
- [24] D. Eriksson, J. Rathsman, and O. Stål, *Comput. Phys. Commun.* **181**, 189 (2010); **181**, 833 (2010).
- [25] J. M. Campbell and R. K. Ellis, *Phys. Rev. D* **60**, 113006 (1999).
- [26] S. Klimenko, J. Konigsberg, and T. M. Liss, Report No. Fermilab-FN-0741, 2003 (unpublished).